Society For Biomaterials

Comparison between alkali heat treatment and sprayed hydroxyapatite coating on thermally-sprayed rough Ti surface in rabbit model: Effects on bone-bonding ability and osteoconductivity

Toshiyuki Kawai,[1] Mitsuru Takemoto,[1] Shunsuke Fujibayashi,[1] Masashi Tanaka,[1] Haruhiko Akiyama,[1] Takashi Nakamura,[2] Shuichi Matsuda[1]

[1]Department of Orthopedic Surgery, Graduate School of Medicine, Kyoto University, Kyoto, Japan
[2]National Hospital Organization Kyoto Medical Center, Kyoto, Japan

Received 28 February 2014; revised 3 July 2014; accepted 1 September 2014
Published online 00 Month 2014 in Wiley Online Library (wileyonlinelibrary.com). DOI: 10.1002/jbm.b.33281

Abstract: In this study, we investigated the effect of different surface treatments (hydroxyapatite (HA) coating, alkali heat treatment, and no treatment) on the ability of bone to bond to a rough arc-sprayed Ti metal surface, using rabbit models. The bone-to-implant contacts for untreated, HA-coated, and alkali heat-treated implants were 21.2%, 72.1%, and 33.8% at 4 weeks, 21.8%, 70.9%, and 30.0% at 8 weeks, and 16.3%, 70.2%, and 29.9% at 16 weeks, respectively (n = 8). HA -coated implants showed significantly higher bone-to-implant contacts than the untreated and alkali heat-treated implants at all the time point, whereas alkali heat-treated implants showed significantly higher bone-to-implant contacts than untreated implants at 4 and 16 weeks. The failure loads in a mechanical test for untreated, HA coated, alkali heat-treated plates were 65.4 N, 70.7 N, and 90.8 N at 4 weeks, 76.1 N, 64.7 N, and 104.8 N at 8 weeks and 88.7 N, 92.6 N, and 118.5 N at 16 weeks, respectively (n = 8). The alkali heat-treated plates showed significantly higher failure loads than HA-coated plates at 8 and 16 weeks. The difference between HA-coated plates and untreated plates were not statistically significant at any time point. Thus HA coating, although it enables high bone-to-implant contact, may not enhance the bone-bonding properties of thermally-sprayed rough Ti metal surfaces. In contrast, alkali heat treatment can be successfully applied to thermally-sprayed Ti metal to enhance both bone-to-implant contact and bone-bonding strength. © 2014 Wiley Periodicals, Inc. J Biomed Mater Res Part B: Appl Biomater 00B: 000–000, 2014.

Key Words: titanium (alloys), hydroxy(1)lapatite, bone ingrowth, orthopaedic, animal model

How to cite this article: Kawai T, Takemoto M, Fujibayashi S, Tanaka M, Akiyama H, Nakamura T, Matsuda S. 2014. Comparison between alkali heat treatment and sprayed hydroxyapatite coating on thermally-sprayed rough Ti surface in rabbit model: Effects on bone-bonding ability and osteoconductivity. J Biomed Mater Res Part B 2014:00B:000–000.

INTRODUCTION

Titanium (Ti) metal and its alloys are widely used in the orthopedic and dental fields because of their high fracture toughness and good biocompatibility. However, they are rarely implanted into a bone defect in their natural form because their bonding to bone can be enhanced by modification of their surface characteristics.[1,2] Various methods have been developed to promote bone in-growth and implant fixation for implants made from Ti metal and its alloys, including physical modification of the implant design,[3] modification of the surface topography,[4–8] and chemical modification of the material composition and structure.[9–12]

Modification of surface topography has been known to influence the bone-bonding ability of the material, promoting bone growth into or onto its structure. Several methods using sintered beads,[4,5] fiber mesh coating,[4] grit blasting,[6,7] or porous metals,[8] have been reported. Fujisawa et al. reported a titanium thermal-spray method known as arc spraying, which provided a rough surface[13] that gave satisfactory results in a monkey model. Subsequently, arc-sprayed artificial joints have been used clinically.

Several methods have been reported to enhance bioactivity of metal implants. One of the best accepted and commercialized bioactive coating materials is plasma-sprayed hydroxyapatite (HA).[9–12] Although many satisfactory clinical results have been reported, there have been several associated problems including fracture of the HA coating,[14] degradation and delamination during long-term implantation.[15] HA particles, when generated near an artificial joint surface, cause third-body wear, leading to excessive polyethylene wear and osteolysis.[15,16] This means that HA-coated implants should be regularly monitored using radiographs for adverse effects such as polyethylene wear and osteolysis.

Kokubo et al. have developed a new technique for obtaining a bioactive surface through alkali and heat

Correspondence to: T. Kawai; e-mail: kawait@kuhp.kyoto-u.ac.jp
Contract grant sponsor: KYOCERA Medical Corporation, Osaka, Japan

TABLE I. Samples Examined in this Study

Sample Type	Shape of Substrate	Thermal Spraying	Additional Treatment
Un-P	Plate	Arc spraying	No
HA-P	Plate	Arc spraying	HA coating
Al-P	Plate	Arc spraying	Alkali heat treatment
Un-C	Cylinder	Arc spraying	No
HA-C	Cylinder	Arc spraying	HA coating
Al-C	Cylinder	Arc spraying	Alkali heat treatment

treatment of titanium metal.[17–21] In an *in vitro* experiment, bone-like apatite was formed in a simulated body fluid (SBF) on a Ti metal surface that had been subjected to the alkali heat treatment. Several articles suggested that Ti metals that have apatite forming ability in simulated body fluid can also form apatite on its surface *in vivo*.[22,23] The bone-bonding ability of a Ti metal plate subjected to this alkali and heat treatment has already been reported.[20,22,24] The treated plate showed significantly higher bone-bonding ability than that of as-abraded Ti metal. However, there has been no study to evaluate the combination of thermal spraying and alkali heat treatment, or to compare the *in vivo* performance of alkali heat treatment and HA coating.

The aim of the present study was to compare the performance (in terms of bone-bonding ability and osteoconductivity) of alkali heat treatment and HA coating on arc-sprayed rough Ti metal using a rabbit model.

MATERIALS AND METHODS

Preparation of plates

Three types of titanium plates (size: 15 × 10 × 2 mm^3) were prepared. Arc-sprayed plate (Un-P) samples were prepared using the inert gas-shielded arc spraying (ISAS) method.[13] The coating material was commercially available pure titanium wire (ASTM F67 Grade 1), manufactured by Shinko Wire Company Ltd. (Hyogo, Japan), with a diameter of 1.6 mm and the substrate was Ti-15Mo-15Zr-3Al alloy (ISO 5832-14), manufactured by Kobe Steel Ltd. (Kobe, Japan). This alloy is currently used in some artificial joints in clinical practice and was chosen as the substrate in this study so that the fabricated plates can have similar compositions to commercially available artificial joints. The titanium wire was melted by arc-discharge heat and the melted titanium was blown onto both sides of the substrate using a high-speed carrier gas.

The target thickness of the ISAS titanium coating was determined to be 300 μm at the peak height, because 300 μm reflects the minimum thickness of the arc-sprayed layer in artificial joints that are already used clinically in Japan. The thickness of the substrate for ISAS coating was 1400 μm so that the total thickness of each plate was 2 mm. After the titanium alloy substrate was coated by the ISAS method in the chamber, it was transferred to a vacuum furnace and heated to 650°C to release residual stress, particularly from the sprayed surface, as described previously.[13]

To prepare plates in group HA-P, after ISAS coating, HA coating was performed using the flame-spray method; the flame was made with acetylene and oxygen gases, and air was used as the high-speed carrier gas for the spray. The target thickness of the HA coating was 20 μm. The HA powder used for this procedure was manufactured by KYOCERA Medical Corporation, Osaka, Japan and was assessed using the criteria of ISO 13779-1; 2008. It had a crystallinity value of 100% relative to the 100% crystalline hydroxyapatite standard value, as determined according to ISO 13779-3. The calcium-to-phosphorus ratio was 1.664 for the atomic ratio and the mass fraction of α-tricalcium phosphate was less than 5%. Specific trace elements, namely arsenic, cadmium, mercury, and lead, were within the maximum allowable limits. The bonding strength of the HA layer made by this method to the Ti metal substrate as well as the bonding strength of the arc-sprayed Ti meal layer to a Ti metal alloy plate was assessed according to ISO 13774-2. It was confirmed that both bonding strengths met the specified criteria and were consistently more than 15 MPa.

To prepare plates in group Al-P, after ISAS coating, an alkali and heat treatment was performed, using the previously reported procedure.[19,25] Briefly, the plates were soaked in a 5.0*M* NaOH aqueous solution at 60°C for 24 h, and then gently washed with distilled water and dried at 40°C for 24 h at room temperature. The plates were subsequently heated to 600°C at a rate of 5°C/min in an electric furnace and held for 1 h before cooling to room temperature. Thirty-four plates were fabricated for each group.

The fabricated samples and their treatments are summarized in Table I. T1

Preparation of cylindrical implants

Three types of cylindrical implants (6 mm diameter, 15 mm long) were also prepared to be used in animal experiments for quantitative histological analysis. Again, the substrate was Ti-15Mo-5Zr-3Al alloy, and the cylinder diameter was 5.4 mm. Arc-sprayed cylindrical bodies (Un-C) were prepared using the same ISAS method as used for the Un-P samples; briefly, for Un-C samples, melted titanium was blown circumferentially onto the surface. The target thickness of the ISAS titanium coating was again 300 μm at peak height, which gave a total diameter of each cylinder of 6 mm.

Group HA-C and Al-C samples were prepared using the same methods as used for HA-P and Al-P, respectively. For group HA-C, the target thickness of the HA coating was 20 μm.

Surface roughness

The surface roughnesses of the plates were evaluated using a profilometer (Form Talysurf PGI+, Taylor-Hobson, Leicester, UK). The arithmetic mean deviation of the profile (Ra) and the maximum average height (Rz) were measured with a cutoff value of 2.5 mm and a measurement length of 12.5 mm, and the drive speed was 0.5 mm/s. For each sample, the average Ra and Rz were computed along ten lines randomly chosen within the individual areas.

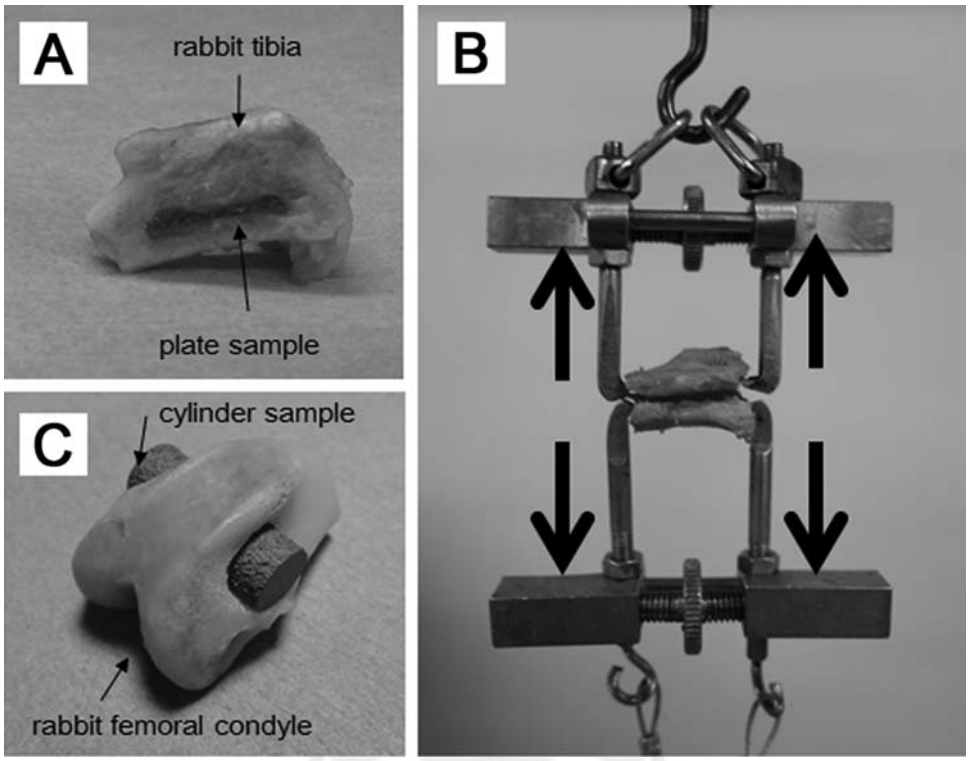

FIGURE 1. Schematic drawings of the detaching test and the preparation for the test. A Insertion of the sample plate into the rabbit tibia. B Tensile load was applied, while holding the anterior and posterior cortices, until detachment occurred. [Color figure can be viewed in the online issue, which is available at wileyonlinelibrary.com.]

AQ2

Scanning electron microscopy and thin-film X-ray diffractometry

The morphologies of the surfaces and cross-sections of the Ti metal plates were examined with a field-emission scanning electron microscope (SEM) (S-4700, Hitachi Ltd., Japan) at an acceleration voltage of 15 kV. For the preparation of cross-section samples, metal plates were embedded in epoxy resin, wet-polished using SiC papers up to #2400 grids, buff-polished with SiO_2 suspension and coated with a thin layer of Au.

The crystalline phases of the surfaces of the Ti metal plates were examined by thin-film X-ray diffraction (TF-XRD; X'Pert PRO MRD, PANalytical Ltd., The Netherlands), using a Cu-Kα X-ray source at 45 kV and 40 mA with a step rate of $2\theta = 0.3^\circ$/min, and a glancing angle of 1° to the incident beam. One plate for each treatment group was used for this analysis.

Assessment of apatite forming ability

The bioactivity of the samples was examined by soaking them in a simulated body fluid (SBF), which had a pH of 7.40, and ion concentrations (mmol/L) of: Na^+, 142.0; K^+, 5.0; Ca^{2+}, 2.5; Mg^{2+}, 1.5; Cl^-, 147.8; HCO^{3-}, 4.2; HPO_4^{2-},1.0; and SO_4^{2-}, 0.5.[26,27] The samples were soaked in 30 mL of the SBF for 3 days at 36.5°C, then removed from the SBF, washed with distilled water, and dried on a clean bench. The formation of apatite on the sample surface was examined using SEM with an attached energy-dispersive X-ray microanalyzer (GENESIS, EDAX Japan, Tokyo, Japan) and also examined by TF-XRD. One plate for each treatment group was used for this analysis.

Animal experiments

Ethic statement. These experiments were carried out in strict accordance with the recommendations in the Guide for the Care and Use of Laboratory Animals of the National Institutes of Health. The protocol was approved by the Animal Research Committee, Graduate School of Medicine, Kyoto University, Japan (Permit Number: Med Kyo 10285). All surgery was performed at the Graduate School of Medicine, Kyoto University. All efforts were made to minimize suffering.

Implantation of plates. The plate implants were rinsed in an isopropylalcohol (IPA) ultrasonic bath for cleaning, sterilized by gamma radiation, and implanted into the proximal tibiae of male Japanese white rabbits ranging in age from 25 to 28 weeks and weighing between 2.8 and 3.2 kg. The surgical methods used have been described previously.[20,28–30] Briefly, the rabbits were anesthetized with an intravenous injection of pentobarbital sodium (0.5 mL/kg), an intramuscular injection of ketamine hydrochloride (10 mg/kg), and local administration of a solution of 0.5% lidocaine. Using aseptic technique, a straight incision of 3 cm was made over the medial side of the knee, and the tibial cortex was exposed. With use of a dental burr, a

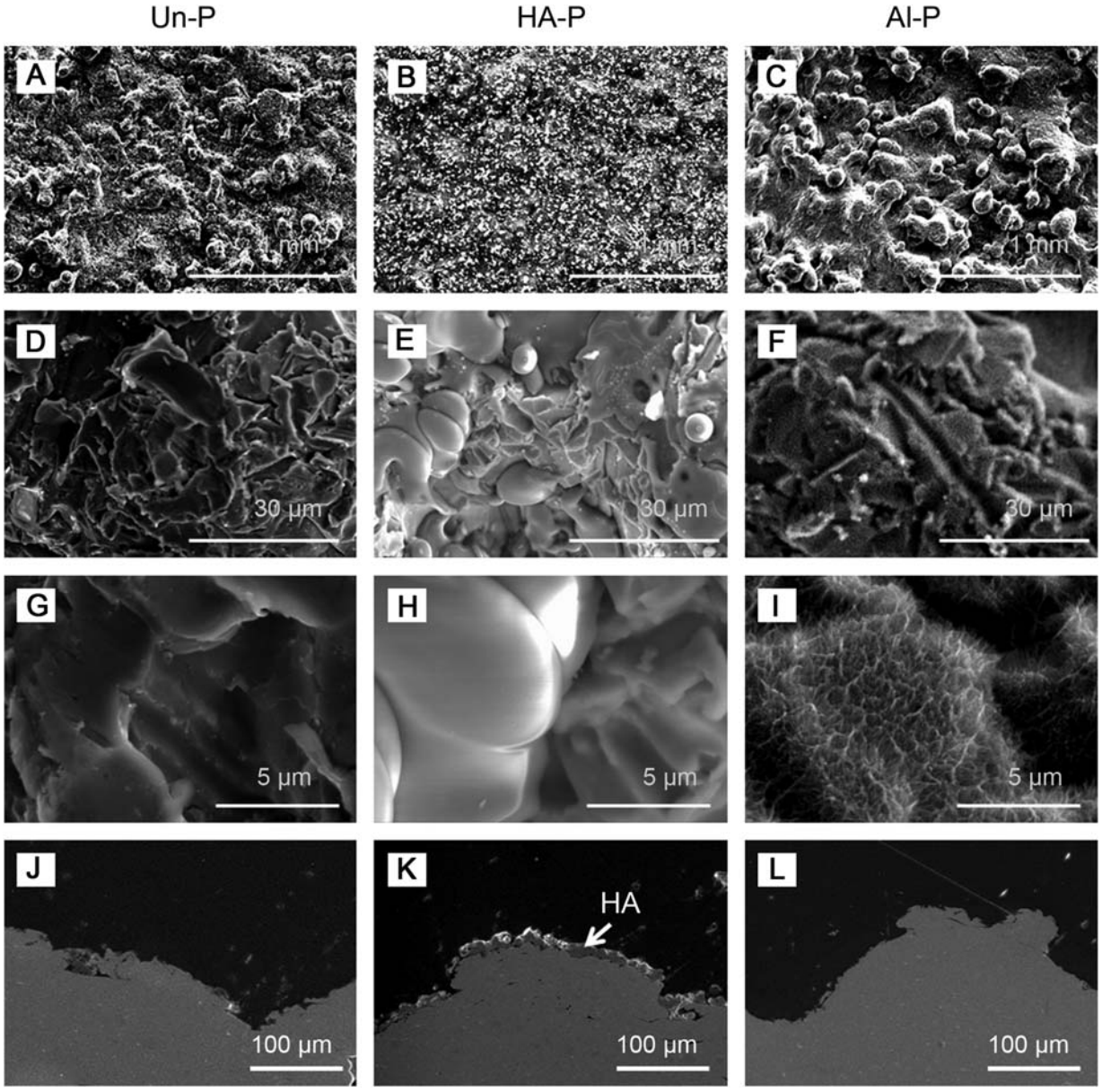

FIGURE 2. SEM images of the surface and cross sections of sample plates. A, D, and G, as-arc-sprayed surface (no additional treatment); B, E, and H, arc-sprayed and HA-coated surface; C, F, and I, arc-sprayed and alkali heat-treated surface; J, cross-section of as-arc-sprayed sample (no further treatment); K, cross-section of arc-sprayed and HA-coated sample; L, cross-section of arc-sprayed and alkali heat-treated sample. [Color figure can be viewed in the online issue, which is available at wileyonlinelibrary.com.]

16 × 2 mm hole was created from the medial to the lateral cortex. Then, the titanium plates were inserted into the hole [Figure 1(a)]. Finally, the wound was closed in layers. The surgical procedures were performed bilaterally. Twelve rabbits were euthanized at 4, 8, or 16 weeks after implantation with a lethal dose of intravenous pentobarbital sodium. Forty-five rabbits were used in this tibial operation. Ten implants were used per experimental condition. Of the 10 implants, eight were used for the detaching tests and the remaining two were analyzed histologically. Based on the excellent bioactivity of chemically and thermally treated titanium that was reported in our previous animal studies,[18,20,31] we hypothesized that statistical differences, or at least broad trends, would be detected among the three types of treatments tested, even if we reduced the number of animals used in this study. Power analysis indicated that a sample size of eight per group would provide 80% statistical power to detect significant differences between the groups ($\alpha = 0.05$, $\beta = 0.20$) using analysis of variance (ANOVA).

Implantation of cylinders. The cylindrical implants were rinsed in an IPA ultrasonic bath for cleaning, sterilized by gamma radiation and implanted into the metaphysis of the femurs of male Japanese white rabbits ranging in age from 25 to 28 weeks and weighing between 2.8 and 3.2 kg, as

shown in Figure1(c). The surgical methods used have been described previously.[32,33] Briefly, the rabbits were anesthetized with an intravenous injection of pentobarbital sodium (0.5 mL/kg) and local administration of a solution of 0.5% lidocaine. Using aseptic technique, a 3 cm skin incision was made over the medial femoral condyle and a 6 mm diameter drill hole was created through the femoral condyles. Then, a cylinder (either Un-C, HA-C, or Al-C treated) was inserted into the hole. The wound was closed in layers. Surgical procedures were performed bilaterally. In a randomized manner, one femur received one implant, while the other femur received a different type of implant. Thirty-six rabbits were used for this femur operation. At each time point (4, 8, and 16 weeks after implantation), 12 rabbits were sacrificed using a lethal dose of intravenous pentobarbital sodium; that is, there were eight implants per experimental condition.

Measurement of detaching failure load. Following euthanasia, segments of the proximal tibia containing the plates were retrieved and prepared for detaching tests. When the newly formed bone was covering the lateral side of the plate and bridging the anterior and posterior bone fragments, the bone tissue on the lateral side of the plate was removed and the anterior and posterior bone fragments were discontinued with a dental burr so that the bridging would not affect the measurement. Traction was applied to each bone segment, at a cross-head speed of 35 mm/min, using an Instron-type autograph (Model 1011, Aikoh Engineering, Nagoya, Japan) [Figure 1(b)]. The traction force and displacement were monitored and the measuring capacity of the load cell equipped with this system was 500 N. When the plate became detached from the bone, the load was recorded as the failure load. When the plate became detached before the detaching test, the failure load was recorded as 0 N. Six samples were examined for each type of implant at each implantation period.

Histological examination. After euthanasia, the implant sites of the femur and tibia were retrieved and then immersed in 10% phosphate-buffered formalin pH 7.25 for 7 days. Those specimens were dehydrated in an ascending series of ethanol concentrations (70%, 80%, 90%, 99%, 100%, and 100% v/v) for 3 days in each and then embedded in polymer resin. Thick sections (250 μm) were cut perpendicular to the implant with a band saw (BS-3000CP, EXACT cutting system, Norderstedt, Germany). Each section was reduced to a final thickness of approximately 40 μm using a grinding-sliding machine (Microgrinding MG-4000, EXACT). The sections were stained with a combination of Stevenel's blue and Van Gieson's picrofuchsin. Histological evaluation was performed on each stained section with a transmission light microscope (Eclipse 80i, Nikon Co., Japan) combined with a digital camera (Nikon Model DS-5M-L1). The observations were mainly performed at the interface between the titanium substrate and the bone

Two 250 μm sections per sample were polished with diamond paper and then coated with a thin layer of carbon for observation by SEM. The SEM observations were also performed at the interface between the titanium substrate and the bone.

Observation of plate surfaces after detaching test. After the detaching test, the surfaces of the plates were prepared for observation. Specimens were washed in sodium hypochlorite solution for removal of the soft tissue, fixed in 10% phosphate-buffered formalin for 3 days. Next they were dehydrated in an ascending series of ethanol concentrations (70%, 80%, 90%, 99%, 100%, and 100% v/v) for 1 day at each concentration. Then those specimens were immersed in isopentyl acetate solution for 1 day and dried in a critical-point drying apparatus (HCP-2, Hitachi, Tokyo, Japan). They were then coated with carbon and analyzed using a SEM with an attached energy-dispersive X-ray microanalyzer (SEM-EDX; EMAX-3000, Horiba, Kyoto, Japan).

Histomorphometric examination. Bone-to-implant contact (%) was measured for cylindrical bodies implanted in femoral condyles and calculated on a personal computer using Adobe Photoshop CS 5 and ImageJ (NIH). Bone-to-implant contact ratio was defined as the fraction of bone in contact with the outer perimeter of the implant. One section was examined for each implant. Thus, eight slices were analyzed for each type of implant for each implantation time.

Statistics

All data are expressed as means ± standard deviation (SD). The homogeneity of the variance among groups at each time point was assessed with the Bartlett test. When the variance was homogeneous, comparisons between groups were performed with one-way ANOVA followed by a *post hoc* test (Tukey–Kramer multiple comparison test). When the variance was not homogeneous, comparisons between groups were performed with the Kruskal–Wallis test followed by a Steel–Dwass *post hoc* test. All analyses were performed using JMP 9 (SAS Institute, Cary, NC).Values of $p < 0.05$ were considered statistically significant.

RESULTS

Structure and phases of surfaces

Scanning electron micrographs of the surfaces and cross-sections of Un-P, HA-P, and Al-P are shown in Figure 2. All three surfaces were rough, and there was a uniform HA layer on the HA-P surface. The high-magnification image shows that there was a submicrometer scale fine network on the surface of the Al-P sample. F2

The XRD patterns of specimens from the three plate groups are shown in Figure 3. As the XRD patterns show, the major phase on the HA-P specimen is hydroxyapatite (HA). The Al-P specimen showed small peaks that were ascribed to rutile and anatase. F3

Surface roughness

The Ra and Rz for each plate were as shown in Figure 4. These indicate that surface roughness decreased after HA F4

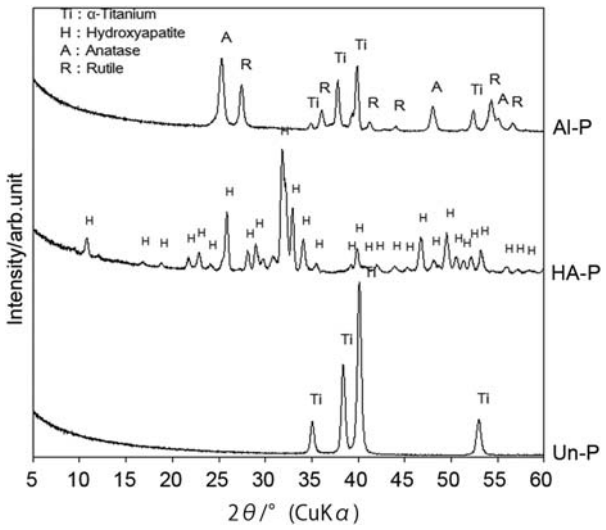

FIGURE 3. TF-XRD patterns of the surfaces of the sample plates.

coating, while alkali heat treatment had little effect on surface roughness.

Apatite formation

F5 Figure 5 shows SEM images of the surfaces of Ti metal samples that had been soaked in SBF for 3 days. No deposits were observed on plates from the Un-P groups, whereas apatite formation was seen on plates from the HA-P and Al-P groups.

Detaching test (failure load)

All rabbits recovered normally from surgery and survived to their predetermined sacrifice date. None of the rabbits showed any evidence of infection, inflammation or dislocation of the implants. The changes in detaching failure loads for each material at 4, 8, and 16 weeks after implantation F6 are summarized in Figure 6. In the following discussion, the failure loads given are means (±standard deviations). At 4 weeks, the bone-bonding strengths of Un-P, HA-P and Al-P were 65.4 N (±9.6), 70.7 N (±8.7) and 90.8 N (±20.8) respectively ($n = 8$). At 8 weeks, they were 76.1 N (±15.9), 64.7 N (±12.3), and 104.8 N (±13.0), and at 16 weeks, 88.7 N (±17.7), 92.6 N (±21.1), and 118.5 N (±26.1) respectively (both $n = 8$).

At 4 weeks, the failure loads of each group were compared by the Kruskal–Wallis test followed by a Steel-Dwass *post hoc* test, because the variances were not homogeneous among those groups (Bartlett: $p = 0.042$), meanwhile, the failure loads were compared by ANOVA followed by a Tukey-Kramer *post hoc* test at 8 and 16 weeks because the variances were considered to be homogeneous (Bartlett: $p = 0.77$ at 8 weeks and $p = 0.61$ at 16 weeks) At 4 weeks, the failure load of Al-P was significantly higher than that of Un-P ($p = 0.027$), but the difference between Al-P and HA-P was not significant ($p = 0.14$). At 8 weeks and at 16 weeks, the failure loads of Al-P were still significantly higher than those of Un-P ($p < 0.0001$ at 8 weeks and $p = 0.049$ at 16 weeks) and HA-P ($p = 0.0012$ at 8 weeks and $p = 0.044$ at 16 weeks). The differences between the failure loads of HA-P and Un-P were not significant at any examined time point ($p = 0.37$ at 4 weeks, $p = 0.24$ at 8 weeks, and $p = 0.96$ at 16 weeks). While the failure loads of Un-P and Al-P increased consistently with time, that of HA-P remained unchanged until 8 weeks, and only then started to increase.

Examination of the bone-plate interface

Representative histological images of each plate sample are shown in Figure 7(A–F). For the samples from the Un-P, F7 HA-P, and Al-P groups, osteocyte-rich new bone had formed in the gap at the implantation site within 4 weeks. Although a large amount of new bone was bound to the surface in all groups, the new bone in the Un-P group had a more woven appearance compared with that in the HA-P and Al-P groups at 4 weeks. The amount of new bone in the vicinity of the plate appeared to be larger in the HA-P and Al-P groups than in the Un-P group. High-magnification images showed that the bone formation on and around the implant was fragmentary and a large portion of the bone tissue was separated from the implant surface by soft tissue. In contrast, the new bone in the HA-P and Al-P groups appeared to contain more thick and contiguous fibers.

Figure 8 shows SEM images of the cross-sections of HA- F8 P implants that had not undergone the detaching test. At 4 weeks, the HA layer on HA-P had become thinner [Figure 8(A,C)] compared with that before implantation [Figure 8(B,D)].

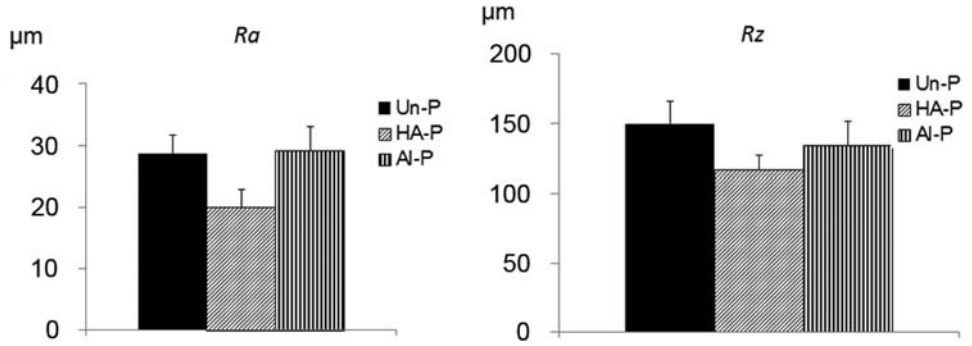

FIGURE 4. Surface roughnesses of the sample plates.

ID: chandrasekar.v Time: 11:03 I Path: N:/3b2/JBMB/Vol00000/140175/APPFile/JW-JBMB140175

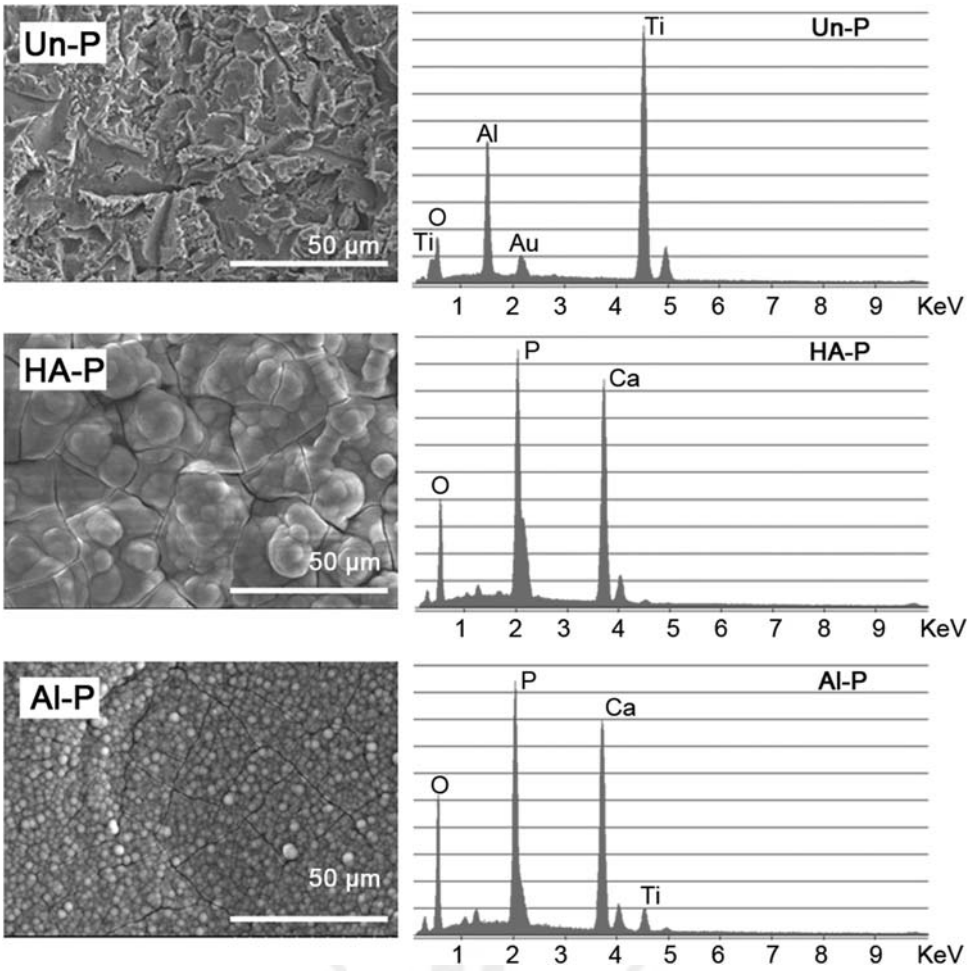

FIGURE 5. SEM images and EDX patterns of the surfaces of the sample plates after soaking in SBF for 3 days. [Color figure can be viewed in the online issue, which is available at wileyonlinelibrary.com.]

SEM observation of detached surface

At 4 weeks, a considerable amount of bone which was well integrated with the rough surface remained on the titanium plate surfaces of groups Un-P, HA-P, and Al-P after the detaching tests [Figure 7(G–I)]. These findings indicate that breakage had occurred mainly in the bone, once bone contact had been established. However, in some parts of the HA-P surface, the bare titanium substrate was observed, implying the delamination of the HA coating during the detaching test. This delamination of HA coating was also observed at 8 and 16 weeks. This phenomenon was confirmed by observation of the cross-sections of the bone-implant interface before and after detaching tests. Before the detaching test, a thin layer of HA coating was observed at 4 weeks after implantation [Figure 9(A)]. However, after the detaching test, the HA layer had disappeared from most of the surface [Figure 9(B)]. On the bone surface after the detaching test, HA coating layers were observed, bound to the bone surface [Figure 9(C,D)]. F9

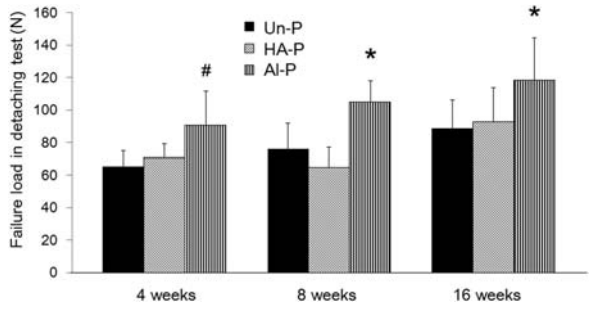

FIGURE 6. Failure load (N) in the detaching test for sample plates after implantation for different periods (error bar: standard deviation). #$p < 0.05$ *vs.* Un-P *$p < 0.05$ *vs.* Un-P and HA-P.

Histological examination of cylindrical implants

Histological images of cylindrical implants and surrounding tissues are shown in Figure 10. At 4 weeks, new bone ongrowth was observed on Un-C, HA-C, and Al-C. Very thin bone tissue was seen covering almost the whole surface of HA-C within the initial 4 weeks [Figure 10(H)], and this layer seemed to remain unchanged at 8 weeks and 16 weeks. This type of thin layer was barely seen on the surface of Un-C or Al-C [Figure 10(G,I)], although robust bone-bonding was observed on the Al-C surface. F10

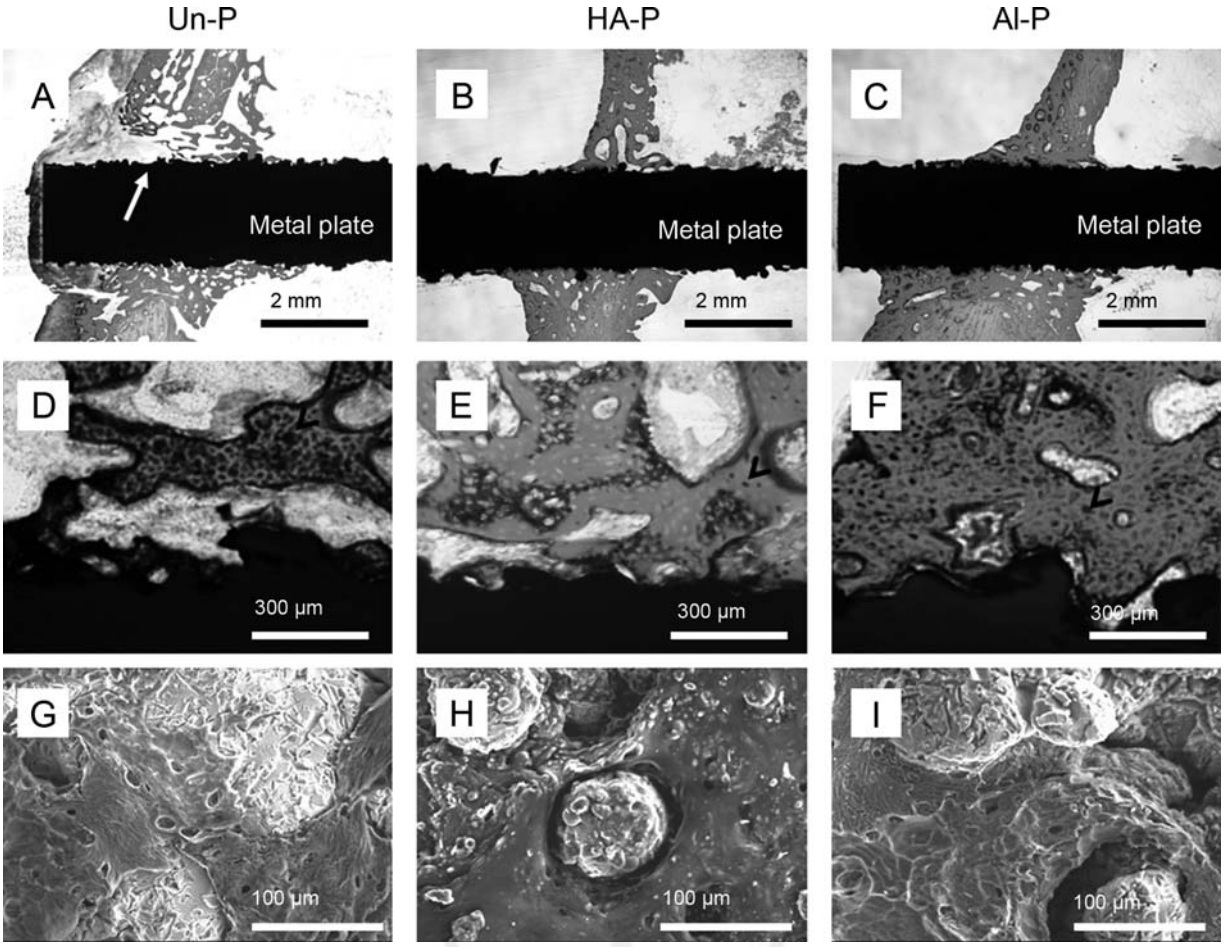

FIGURE 7. A–F, Nondecalcified histological sections of each plate implant 4 weeks after implantation: A and D Un-P, B and E HA-P, C and F Al-P. Stains: Stevenel's blue and Van Gieson's picrofuchsin. The white arrow indicates a gap between the plate and new bone and black arrow heads indicate osteocyte. G–I, SEM images of the surface of each plate after the detaching test, 4 weeks after implantation. G, Un-P; H, HA-P; I, Al-P. [Color figure can be viewed in the online issue, which is available at wileyonlinelibrary.com.]

Bone-to-implant contact

Bone-to-implant contact area ratio for Un-C, HA-C, and Al-C were 21.2 (±7.3), 72.1 (±12.1), and 33.8 (±10.2) % at 4 weeks, 21.8 (±5.7), 70.9 (±12.1), and 30.0 (±7.1) % at 8 weeks and 16.3 (±5.3), 70.2 (±9.2), and 29.9 (±7.7) % at 16 weeks, respectively (Figure 11).

Using the Bartlett test, homogeneity of variance was confirmed for each time point and therefore ANOVA and a Tukey–Kramer multiple comparison test were used for statistical analyses. Bone-to-implant contact ratio for the Al-P was significantly higher than that for the Un-P at 4 and 16 weeks ($p = 0.048$ at 4 weeks and $p = 0.0045$ at 16 weeks), whereas the difference at 8 weeks was not statistically significant ($p = 0.16$). At every time point, the bone-to-implant contact ratio was significantly higher for the HA-P group implants than for the Al-P or Un-P groups ($p < 0.0001$).

DISCUSSION

In this study, we examined the effects of additional surface treatments to thermal-sprayed titanium metal, in terms of bone-bonding ability and bone-to-implant contact ratio. The detachment tests and histological observations described above showed that arc-sprayed Ti metal, even without additional surface treatment, has high bone-bonding ability as early as 4 weeks after implantation. The failure load for the arc-sprayed plate (Un-P) was around 60 N at 4 weeks, whereas the failure load previously reported for alkali and heat-treated flat Ti metal plate was 12.7 N[20] while that for mixed-acid and heat-treated flat Ti metal plate was 14.0 N.[34] It is well accepted that titanium metals with rough surfaces can achieve osseointegration.[35–37] The high bone-bonding ability of Un-P, therefore, can be attributed to its rough surface structure.

Arc-sprayed and alkali-heat-treated plates (Al-P) showed higher failure loads than Un-P at every time point. This indicates that alkali heat treatment can be effectively applied, even to surfaces with complex structures, such as arc-sprayed titanium metal, and that this treatment further enhances bone-bonding ability. How alkali heat treatment enhances the bone-bonding ability of Ti metal has been already discussed elsewhere.[17–19,21] Alkali heat-treated Ti has apatite forming ability in SBF. The *in vivo* bioactivity of biomaterials was reported to be precisely mirrored by their *in vitro* apatite forming ability in SBF.[27] Therefore, alkali heat-treated Ti presumably formed apatite also *in vivo*,

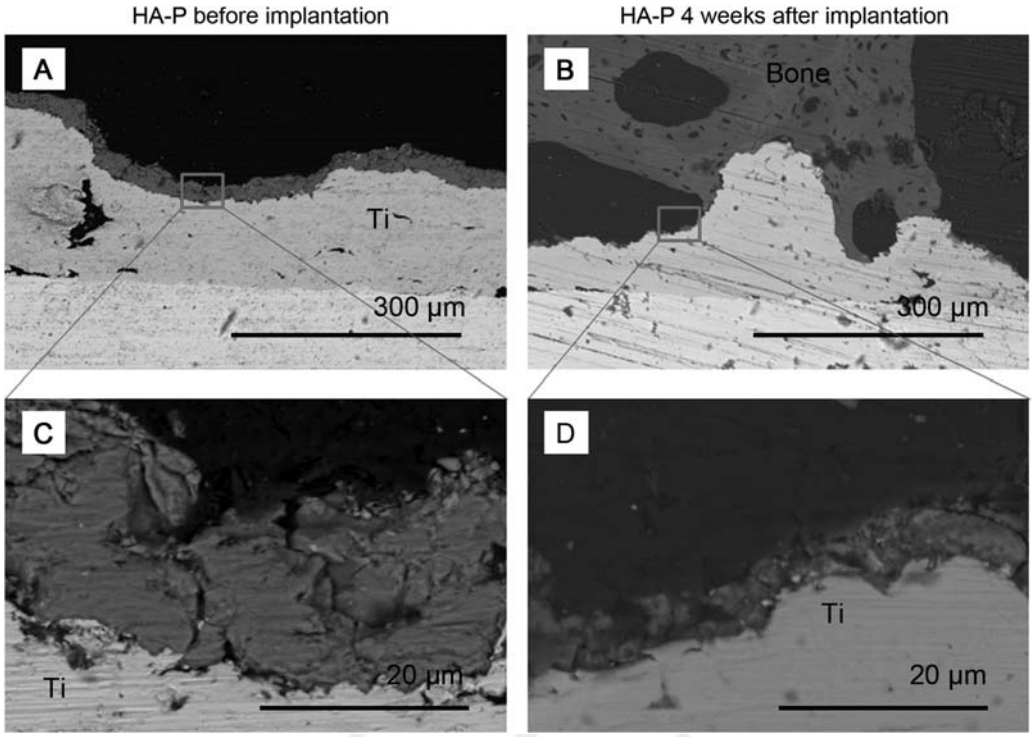

FIGURE 8. SEM images of the cross sections of HA-P specimens: A and C, Before implantation; B and D, after implantation for 4 weeks; C, high magnification image of area indicated by white rectangle in a; D, high magnification image of area indicated by red rectangle in B. [Color figure can be viewed in the online issue, which is available at wileyonlinelibrary.com.]

which is a driving force for bone-bonding, although we did not confirm apatite formation *in vivo* in this study. The present study confirmed that alkali heat treatment also further enhanced the bone-bonding ability of arc-sprayed Ti metal.

The arc-sprayed and alkali heat-treated cylindrical implants (Al-C) showed higher bone-to-implant contact than seen for the Un-C samples and the difference was significant at 4 and 16 weeks. This result was generally consistent with previous reports on the enhanced bone-to-implant contact of alkali heat-treated Ti metal,[23,32] although the difference between untreated and alkali heat-treated implants appeared more marked in those studies. For example, Takemoto et al.[32] reported increased bone-to-implant contact in rabbit femoral condyle using porous titanium implants that had been alkali heat treated. The bone-to-implant contact of their untreated and alkali heat-treated implants were 10.5% and 13.5% at 2 weeks, 12.7% and 16.7% at 4 weeks, 10.2% and 17.7% at 8 weeks, and 7.8% and 19.2% at 16 weeks, respectively. However, while in that report the bone-to-implant contact was analyzed for the entire inner structure of the porous body, only the contact at the outer circumference of the body was analyzed in this study. Nishiguchi et al.[23] reported the bone-to-implant contact of a smooth untreated Ti metal rod and an alkali heat-treated Ti metal rod as 9.5% and 30.1% at 3 weeks, 14.0% and 39.2% at 6 weeks, and 19.2% and 55.8% at 12 weeks, respectively. Their rods were inserted into the femoral medullary canal and press-fit to the endosteal surface of the cortex, while in the present study the implant was inserted into the trabecular bone in the femoral condyle. In addition, the control group used in the study was an untreated smooth Ti metal, whereas the control group in the present study had the rough arc-sprayed surface. These differences may explain why a more marked difference in bone-to-implant contact was observed in Nishiguchi et al.'s study.

HA-coated cylindrical implants (HA-C) showed significantly more bone-to-implant contact than that seen for Al-C. The bone-to-implant contact for HA-C in this study, ($72.1 \pm 12.1\%$ at 4 weeks, $70.9 \pm 12.1\%$ at 8 weeks, $70.2 \pm 9.2\%$ at 16 weeks, was consistent with previous studies. Peraire et al.[38] reported that HA plasma sprayed implants showed bone-implant contact of 67%, while HA pulsed-laser-deposited implants showed contact of 86% after 26 weeks in rabbit tibiae. According to Eom et al.,[39] a HA coated implants had bone-to-implant contact of 79.24% at 4 weeks and 85.97% at 8 weeks in the mandible of miniature pigs.

HA-related bone formation is believed to begin with surface dissolution of the HA, which releases calcium and phosphate ions into the space around the implant. Reprecipitation of carbonated apatite then occurs on the coating surface.[40] The HA binds serum proteins and cellular integrin receptors, allowing osteoblastic cells to bind to the surface.[41,42] Bone formation follows at both the bone and coating surfaces.[43] In this study, a thin layer of new bone spread to cover almost all the surface of the HA-C implants within 4 weeks of implantation (Figure 10); this layer remained at 16 weeks, indicating the strong osteoconductivity of HA.

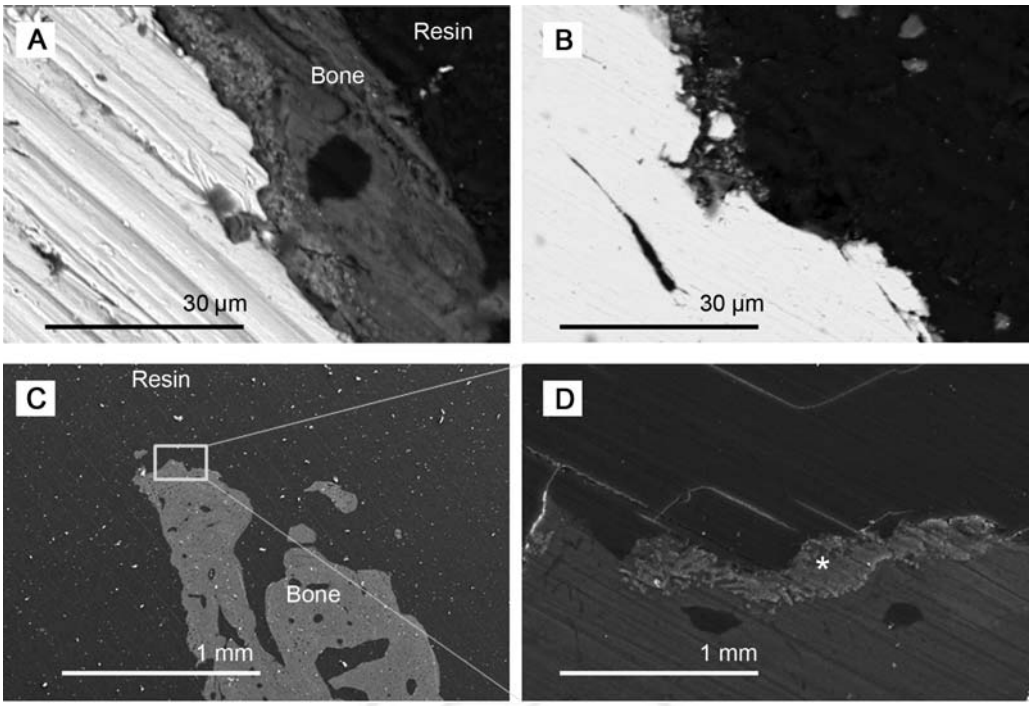

FIGURE 9. SEM images of the cross sections of: A, HA-P specimen 4 weeks after implantation; B, HA-P specimen after the detaching test, 4 weeks after implantation; C, bone detached from HA-P plate 4 weeks after implantation; D, high magnification image of area indicated by red rectangle in C, *hydroxyapatite fragment. [Color figure can be viewed in the online issue, which is available at wileyonlinelibrary.com.]

However, HA-coated plates (HA-P) showed significantly lower failure loads than alkali heat-treated plates (Al-P) at 8 and 16 weeks and there was no statistically significant difference between the failure loads of the HA-P and Un-P implants at any time point. The unexpectedly low failure loads of HA-coated plates may be because of the lower surface roughness and mechanical strength of the HA layer. Firstly, the Ra and Rz of HA-P were lower than those of Un-P and Al-P, presumably because plasma spraying of HA affected the surface topography of the arc-sprayed titanium metal. This decrease in surface roughness might have undermined the bone-bonding, because the surface roughness is known to be a strong contributor to osseointegration.[44] Secondly, at as early as 4 weeks, the HA coating layer observed by SEM was thinner than 20 μm [Figure 8(b,d)]. Resorption of the HA layer might have affected the mechanical properties of the HA layer, and resulted in lower failure loads in the detachment tests. Observation of the plate surfaces after detachment tests revealed that the HA layer had detached from the implant and was stuck to the bone surface (Figure 9). However, despite the decrease in thickness, the bone-to-implant contact of HA-C remained very high at 8 weeks and at 16 weeks (Figure 11).

The discrepancy between the bone-implant contacts and the mechanical test results can also be ascribed to the implant sites. Different performances of implants have sometimes been reported in different bone types. Some authors suggested that bone-to-implant contact should be separately calculated for the cortical region and endosteal region in a rabbit model.[45] Previous authors proposed insertion of implants into the tibia of rabbits,[46] while other authors suggested the femoral condyle.[47] The structure of the femoral condyle mainly consists of trabecular bone, while the tibia is composed of cortical bone and the endosteal space. We cannot rule out the possibility that this difference between the femoral condyle and the tibia might have resulted in the discrepancy between the bone-to-implant contacts and failure loads.

In this study, the failure load of HA-P did not increase from 4 weeks to 8 weeks whereas that of Un-P and Al-P increased steadily. These findings were not consistent with previous studies.[39,48,49] In those reports, mechanical testing showed significantly higher implant-bone bonding for apatite layer-coated implants[48] and HA-coated implants[39,49] than for uncoated Ti implants. However, Fuming et al.[47] reported that the removal torques of calcium phosphate (Ca-P)-coated Ti implants did not differ significantly from those of uncoated Ti implants at 2 and 4 weeks. In addition, the removal torque of the Ca-P coated implants was significantly lower than that of the uncoated implants at 6 weeks, and they ascribed the low mechanical data at 6 weeks to absorbance of the Ca-P layer. Fontana et al.[50] also found that there was no significant difference between Ca-P-coated and uncoated Ti implants in removal torque tests. Specifically, the removal torque for the Ca-P-coated implants was 30.28 ± 9.41 N at 4 weeks, but it decreased to 20.16 ± 3.03 N at 9 weeks, and the authors stated that the low mechanical data for the Ca-P coated implants at 9 weeks may be attributed to fast dissolution of the Ca-P coating. This would also imply that the HA layer in the present study was

ID: chandrasekar.v Time: 11:03 I Path: N:/3b2/JBMB/Vol00000/140175/APPFile/JW-JBMB140175

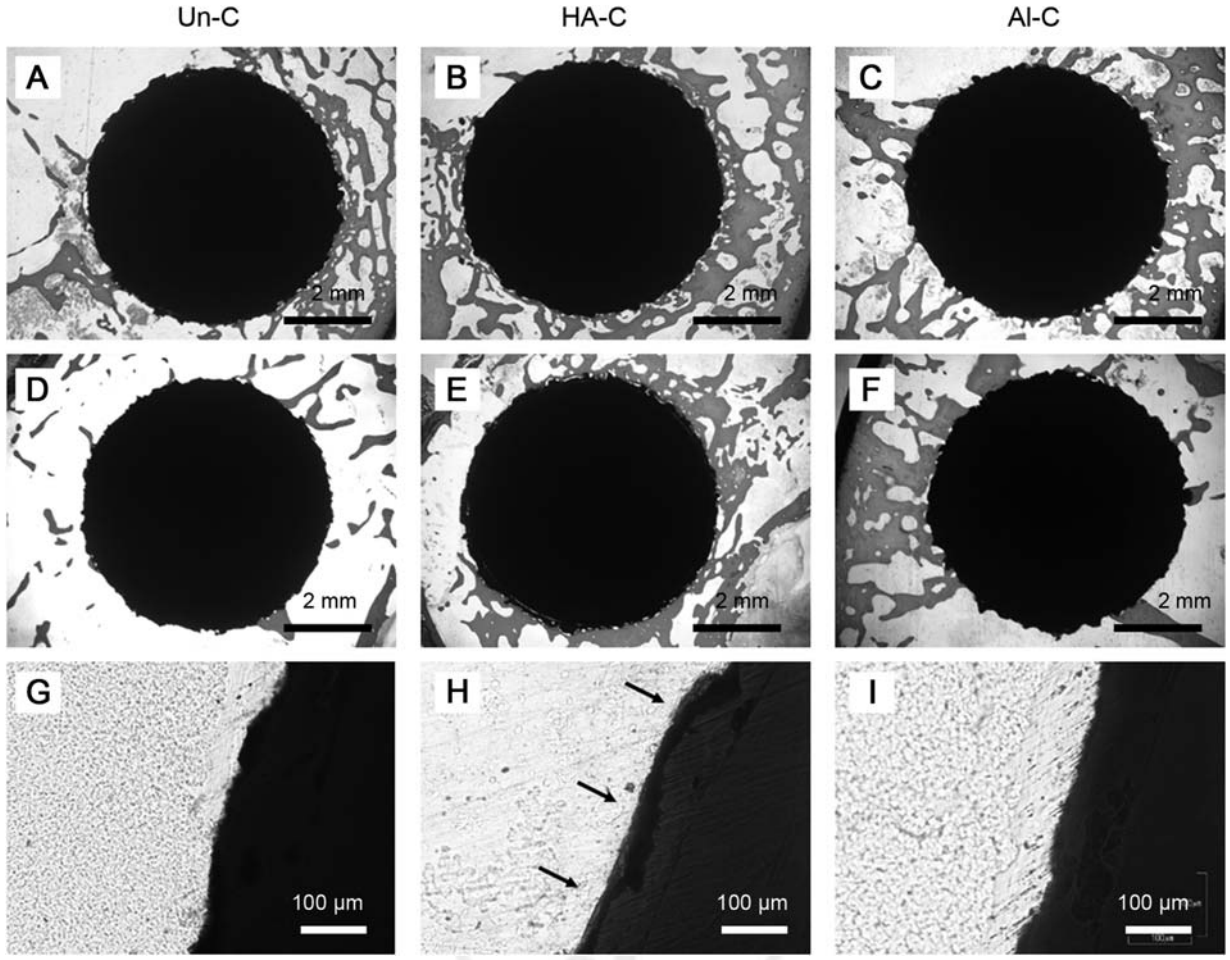

FIGURE 10. Nondecalcified histological sections of each cylinder implant at different periods after implantation: A–C, G–I, 4 weeks; D–F, 16 weeks. A, D, and G, Un-C; B, E, and H, HA-C; C, F, and I, Al-C. Stains: Stevenel's blue and Van Gieson's picrofuchsin. G–I, High magnification images of each specimen 4 weeks after implantation. Black arrows indicate a thin bone layer covering the surface of HA-C. [Color figure can be viewed in the online issue, which is available at wileyonlinelibrary.com.]

gradually absorbed, thereby making the bonding of the HA layer to Ti metal less stable at 8 weeks.

Hydroxyapatite coating is widely used in dental implants and orthopaedic prostheses. Although it has been observed that an HA coating improves early fixation in bone,[39,45,51–53] recent clinical orthopedic studies have indicated that there is no clear advantage in using an HA coating, for either a femoral stem or an acetabular cup in hip implants.[54–58] Some of the major concerns associated with a plasma-sprayed coating are possible delamination of the coating from the Ti implant surface and failure at the implant-coating interface, although the coating is well attached to the bone tissue. Differences in the dissolution rates between the various phases that comprise the coating may result in delamination, particle release and, ultimately, clinical failure of the implant.[59–61] In this study, the plasma-sprayed HA surface showed higher bone-to-implant contact in histological examination than seen for either the as-sprayed (Un-C) or arc-sprayed and alkali heat-treated (Al-C) samples; however, the alkali heat-treated surface showed higher failure loads in mechanical tests. These finding are consistent with the previous studies, which implies that although HA coating still may find wide clinical application, alkali heat treatment can be more successfully used for titanium implants in conditions where the interface between the implant and bone is subjected to higher mechanical stress.

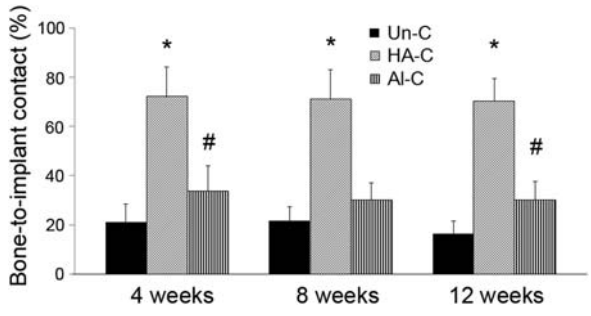

FIGURE 11. Histomorphometric results for the bone-to-implant contact. *$p < 0.05$ *vs.* Un-C and Al-H, #$p < 0.05$ *vs.* Un-C and HA-C.

There are several limitations to this study. First, although the traction force was applied to the bone-implant

interface in the detaching test, more complex and varied loadings would be applied to the surface of an artificial joint. This is a weakness of the present study. Second, the bone-bonding was evaluated in tibiae and the bone-to-implant contact was measured in femoral condyles. These two sites have different bone types, which makes it difficult to directly compare the results of the detaching test and bone-to-implant contact. Third, the number of plate sample use for histological analysis ($n = 2$) was too small to conclude that the tendencies and characteristics of the bone formation were consistent. Finally, the follow-up period in this study was up to 16 weeks. To discuss and anticipate the long term results, longer follow-up periods will be needed.

CONCLUSIONS

In this study, we compared the effects of different surface treatments (HA coating, alkali heat treatment, and no treatment) on the bone-bonding property and bone-implant contact of arc-sprayed Ti metal surfaces, using rabbit models. Both HA coating and alkali heat treatment showed significantly higher bone-implant contact in rabbit femurs than found for the untreated samples. HA-coated samples showed significantly higher bone-to-implant contact than alkali heat-treated samples at 4, 8, and 16 weeks. However, alkali heat-treated samples showed stronger bone-bonding than HA-coated samples at 8 and 16 weeks. The difference in bone-bonding strength between HA-coated samples and untreated samples was not statistically significant at any of the time points examined. This could be attributable to absorbance of the HA layer, which would consequently weaken the bonding of the HA layer to Ti metal. Thus, the present study demonstrates that alkali heat treatment can be successfully applied to Ti metal with modified surface topography and further enhance the bone-bonding and bone-to-implant contact.

REFERENCES

1. Head WC, Bauk DJ, Emerson RH, Jr. Titanium as the material of choice for cementless femoral components in total hip. Clin Orthop Relat Res 1995:85–90.
2. Lester DK. Microscopic studies of human press fit titanium hip prostheses. Clin Orthop Relat Res 1997:143–150.
3. Khanuja HS, Vakil JJ, Goddard MS, Mont MA. Cementless femoral fixation in total hip arthroplasty. J Bone Joint Surg Am 2011; 93:500–509.
4. Bourne RB, Rorabeck CH, Burkart BC, Kirk PG. Ingrowth surfaces. Plasma spray coating to titanium alloy hip replacements. Clin Orthop Relat Res 1994:37–46.
5. Pilliar RM. Powder metal-made orthopedic implants with porous surface for fixation by tissue. Clin Orthop Relat Res 1983:42–51.
6. Zweymuller KA, Lintner FK, Semlitsch MF. Biologic fixation of a press-fit titanium hip joint endoprosthesis. Clin Orthop Relat Res 1988:195–206.
7. Hacking SA, Bobyn JD, Tanzer M, Krygier JJ. The osseous response to corundum blasted implant surfaces in a canine hip model. Clin Orthop Relat Res 1999:240–253.
8. Bobyn JD, Stackpool GJ, Hacking SA, Tanzer M, Krygier JJ. Characteristics of bone ingrowth and interface mechanics of a new porous tantalum. J Bone Joint Surg Br 1999;81:907–914.
9. Yee AJ, Kreder HK, Bookman I, Davey JR. A randomized trial of hydroxyapatite coated prostheses in total hip arthroplasty. Clin Orthop Relat Res 1999:120–132.
10. McNally SA, Shepperd JA, Mann CV, Walczak JP. The results at nine to twelve years of the use of a hydroxyapatite-coated femoral. J Bone Joint Surg Br 2000;82:378–382.
11. Geesink RG, Hoefnagels NH. Six-year results of hydroxyapatite-coated total hip replacement. J Bone Joint Surg Br 1995;77:534–547.
12. Moroni A, Toksvig-Larsen S, Maltarello MC, Orienti L, Stea S, Giannini S. A comparison of hydroxyapatite-coated, titanium-coated, and uncoated tapered. J Bone Joint Surg Am 1998;80: 547–554.
13. Fujisawa A, Noda I, Nishio Y, Okimatsu H. The development of new titanium arc-sprayed artificial joints. Mater Sci Eng C 1995;2: 151–157.
14. de Groot K, Geesink R, Klein CP, Serekian P. Plasma sprayed coatings of hydroxylapatite. J Biomed Mater Res 1987;21:1375–1381.
15. Bloebaum RD, Beeks D, Dorr LD, Savory CG, DuPont JA, Hofmann AA. Complications with hydroxyapatite particulate separation in total hip arthroplasty. Clin Orthop Relat Res 1994:19–26.
16. Morscher EW, Hefti A, Aebi U. Severe osteolysis after third-body wear due to hydroxyapatite particles from acetabular cup coating. J Bone Joint Surg Br 1998;80:267–272.
17. Kokubo T, Miyaji F, Kim H-M, Nakamura T. Spontaneous formation of bonelike apatite layer on chemically treated titanium metals. J Am Ceramic Soc 1996;79:1127–1129.
18. Nishiguchi S, Kato H, Fujita H, Kim HM, Miyaji F, Kokubo T, et al. Enhancement of bone-bonding strengths of titanium alloy implants by alkali and heat treatments. J Biomed Mater Res 1999; 48:689–96. AQ1
19. Nishiguchi S, Nakamura T, Kobayashi M, Kim HM, Miyaji F, Kokubo T. The effect of heat treatment on bone-bonding ability of alkali-treated titanium. Biomaterials 1999;20:491–500.
20. Fujibayashi S, Nakamura T, Nishiguchi S, Tamura J, Uchida M, Kim HM, et al. Bioactive titanium: effect of sodium removal on the bone-bonding ability of bioactive titanium prepared by alkali and heat treatment. J Biomed Mater Res 2001;56:562–570.
21. Nishiguchi S, Kato H, Fujita H, Oka M, Kim HM, Kokubo T, et al. Titanium metals form direct bonding to bone after alkali and heat treatments. Biomaterials 2001;22:2525–2533.
22. Yan WQ, Nakamura T, Kobayashi M, Kim HM, Miyaji F, Kokubo T. Bonding of chemically treated titanium implants to bone. J Biomed Mater Res 1997;37:267–275.
23. Nishiguchi S, Fujibayashi S, Kim HM, Kokubo T, Nakamura T. Biology of alkali- and heat-treated titanium implants. J Biomed Mater Res A 2003;67:26–35.
24. Kato H, Nakamura T, Nishiguchi S, Matsusue Y, Kobayashi M, Miyazaki T, et al. Bonding of alkali- and heat-treated tantalum implants to bone. J Biomed Mater Res 2000;53:28–35.
25. Kim HM, Miyaji F, Kokubo T, Nakamura T. Effect of heat treatment on apatite-forming ability of Ti metal induced by alkali. J Mater Sci Mater Med 1997;8:341–347.
26. Kokubo T, Kushitani H, Sakka S, Kitsugi T, Yamamuro T. Solutions able to reproduce in vivo surface-structure changes in bioactive glass-ceramic A-W. J Biomed Mater Res 1990;24:721–734.
27. Kokubo T, Takadama H. How useful is SBF in predicting in vivo bone bioactivity? Biomaterials 2006;27:2907–2915.
28. Nakamura T, Yamamuro T, Higashi S, Kokubo T, Itoo S. A new glass-ceramic for bone replacement: Evaluation of its bonding to bone tissue. J Biomed Mater Res 1985;19:685–698.
29. Takemoto M, Fujibayashi S, Neo M, Suzuki J, Kokubo T, Nakamura T. Bone-bonding ability of a hydroxyapatite coated zirconia-alumina nanocomposite with a microporous surface. J Biomed Mater Res A 2006;78:693–701.
30. Onishi E, Fujibayashi S, Takemoto M, Neo M, Maruyama T, Kokubo T, et al. Enhancement of bone-bonding ability of bioactive titanium by prostaglandin E2 receptor selective agonist. Biomaterials 2008;29:877–883.
31. Fujibayashi S, Neo M, Kim HM, Kokubo T, Nakamura T. Osteoinduction of porous bioactive titanium metal. Biomaterials 2004;25: 443–450.
32. Takemoto M, Fujibayashi S, Neo M, Suzuki J, Kokubo T, Nakamura T. Mechanical properties and osteoconductivity of porous bioactive titanium. Biomaterials 2005;26:6014–6023.

33. Kawai T, Takemoto M, Fujibayashi S, Akiyama H, Yamaguchi S, Pattanayak DK, et al. Osteoconduction of porous Ti metal enhanced by acid and heat treatments. J Mater Sci Mater Med 2013;24:1707–1715.
34. Kawai T, Takemoto M, Fujibayashi S, Neo M, Akiyama H, Yamaguchi S, et al. Bone-bonding properties of Ti metal subjected to acid and heat treatments. J Mater Sci Mater Med 2012; 23:2981–2992.
35. Feighan JE, Goldberg VM, Davy D, Parr JA, Stevenson S. The influence of surface-blasting on the incorporation of titanium-alloy implants in a rabbit intramedullary model. J Bone Joint Surg Am 1995;77:1380–1395.
36. Wong M, Eulenberger J, Schenk R, Hunziker E. Effect of surface topology on the osseointegration of implant materials in trabecular bone. J Biomed Mater Res 1995;29:1567–1575.
37. Hacking SA, Harvey EJ, Tanzer M, Krygier JJ, Bobyn JD. Acid-etched microtexture for enhancement of bone growth into porous-coated implants. J Bone Joint Surg Br 2003;85:1182–1189.
38. Peraire C, Arias JL, Bernal D, Pou J, Leon B, Arano A, et al. Biological stability and osteoconductivity in rabbit tibia of pulsed laser deposited hydroxylapatite coatings. J Biomed Mater Res A 2006;77:370–379.
39. Eom TG, Jeon GR, Jeong CM, Kim YK, Kim SG, Cho IH, et al. Experimental study of bone response to hydroxyapatite coating implants: bone-implant contact and removal torque test. Oral Surg Oral Med Oral Pathol Oral Radiol 2012;114:411–418.
40. LeGeros RZ. Properties of osteoconductive biomaterials: Calcium phosphates. Clin Orthop Relat Res 2002:81–98.
41. Kilpadi KL, Chang PL, Bellis SL. Hydroxylapatite binds more serum proteins, purified integrins, and osteoblast precursor cells than titanium or steel. J Biomed Mater Res 2001;57:258–267.
42. Porter AE, Hobbs LW, Rosen VB, Spector M. The ultrastructure of the plasma-sprayed hydroxyapatite-bone interface predisposing to bone bonding. Biomaterials 2002;23:725–733.
43. Sun L, Berndt CC, Gross KA, Kucuk A. Material fundamentals and clinical performance of plasma-sprayed hydroxyapatite coatings: A review. J Biomed Mater Res 2001;58:570–592.
44. Hacking SA, Tanzer M, Harvey EJ, Krygier JJ, Bobyn JD. Relative contributions of chemistry and topography to the osseointegration of hydroxyapatite coatings. Clin Orthop Relat Res 2002:24–38.
45. Meirelles L, Arvidsson A, Andersson M, Kjellin P, Albrektsson T, Wennerberg A. Nano hydroxyapatite structures influence early bone formation. J Biomed Mater Res A 2008;87:299–307.
46. Suh JY, Jeung OC, Choi BJ, Park JW. Effects of a novel calcium titanate coating on the osseointegration of blasted endosseous implants in rabbit tibiae. Clin Oral Implants Res 2007;18:362–369.
47. Fuming H, Guoli Y, Xiaoxiang W, Shifang Z. The removal torque of titanium implant inserted in rabbit femur coated with biomimetic deposited Ca-P coating. J Oral Rehabil 2008;35:754–765.
48. Yan WQ, Nakamura T, Kawanabe K, Nishigochi S, Oka M, Kokubo T. Apatite layer-coated titanium for use as bone bonding implants. Biomaterials 1997;18:1185–1190.
49. Yamada M, Ueno T, Tsukimura N, Ikeda T, Nakagawa K, Hori N, et al. Bone integration capability of nanopolymorphic crystalline hydroxyapatite coated on titanium implants. Int J Nanomedicine 2012;7:859–873.
50. Fontana F, Rocchietta I, Addis A, Schupbach P, Zanotti G, Simion M. Effects of a calcium phosphate coating on the osseointegration of endosseous implants in a rabbit model. Clin Oral Implants Res 2011;22:760–766.
51. Yin K, Wang Z, Fan X, Bian Y, Guo J, Lan J. The experimental research on two-generation BLB dental implants - part I: surface modification and osseointegration. Clin Oral Implants Res 2012; 23:846–852.
52. Faeda RS, Spin-Neto R, Marcantonio E, Guastaldi AC, Marcantonio E, Jr. Laser ablation in titanium implants followed by biomimetic hydroxyapatite coating: Histomorphometric study in rabbits. Microsc Res Tech 2012;75:940–948.
53. Grandfield K, Palmquist A, Goncalves S, Taylor A, Taylor M, Emanuelsson L, et al. Free form fabricated features on CoCr implants with and without hydroxyapatite coating in vivo: a comparative study of bone contact and bone growth induction. J Mater Sci Mater Med 2011;22:899–906.
54. Lazarinis S, Karrholm J, Hailer NP. Effects of hydroxyapatite coating on survival of an uncemented femoral stem. A Swedish Hip Arthroplasty Register study on 4,772 hips. Acta Orthop 2011;82: 399–404.
55. Lazarinis S, Karrholm J, Hailer NP. Increased risk of revision of acetabular cups coated with hydroxyapatite. Acta Orthop 2010;81: 53–59.
56. Camazzola D, Hammond T, Gandhi R, Davey JR. A randomized trial of hydroxyapatite-coated femoral stems in total hip arthroplasty: a 13-year follow-up. J Arthroplasty 2009;24:33–37.
57. Gandhi R, Davey JR, Mahomed NN. Hydroxyapatite coated femoral stems in primary total hip arthroplasty: A meta-analysis. J Arthroplasty 2009;24:38–42.
58. Stilling M, Rahbek O, Soballe K. Inferior survival of hydroxyapatite versus titanium-coated cups at 15 years. Clin Orthop Relat Res 2009;467:2872–2879.
59. Le Guehennec L, Soueidan A, Layrolle P, Amouriq Y. Surface treatments of titanium dental implants for rapid osseointegration. Dent Mater 2007;23:844–854.
60. Tinsley D, Watson CJ, Russell JL. A comparison of hydroxylapatite coated implant retained fixed and removable mandibular prostheses over 4 to 6 years. Clin Oral Implants Res 2001;12:159–166.
61. Wheeler SL. Eight-year clinical retrospective study of titanium plasma-sprayed and hydroxyapatite-coated cylinder implants. Int J Oral Maxillofac Implants 1996;11:340–350.